Article

A Cycloaddition Cascade Approach to the Total Synthesis of (−)-FR182877

David A. Evans, and Jeremy T. Starr

More About This Article

Additional resources and features associated with this article are available within the HTML version:

- Supporting Information
- Links to the 2 articles that cite this article, as of the time of this article download
- Access to high resolution figures
- Links to articles and content related to this article
- Copyright permission to reproduce figures and/or text from this article

View the Full Text HTML

A Cycloaddition Cascade Approach to the Total Synthesis of (−)-FR182877

David A. Evans* and Jeremy T. Starr

Contribution from the Department of Chemistry and Chemical Biology, Harvard University, Cambridge, Massachusetts 02138

Received July 30, 2003; E-mail: evans@chemistry.harvard.edu

Abstract: An asymmetric synthesis of the cytotoxic natural product, (−)-FR182877 (**1**), has been achieved. Chirality for the entire structure was established using two (4R)-4-benzyl-2-oxazolidinone-mediated boron aldol reactions. A 19-membered macrocarbocycle was synthesized by the coupling of two fragments using a regioselective Suzuki coupling (**17** + **23** → **26**; 84%) and macrocyclization of a β-keto ester (**30** → **31**; 77%). Oxidation of **31** triggered a sequence of stereoselective transannular Diels−Alder reactions (**32** → **34**; 63%) forming four new rings and seven new stereocenters in the pivotal construction event. This pentacyclic intermediate was subsequently transformed to (−)-FR182877. Semiempirical calculations of the transannular Diels−Alder cycloaddition cascade were carried out to determine the origins of asymmetric induction.

Introduction

Background. In 1998, Sato and co-workers reported a new cytotoxic natural product (WS9885B), isolated from *Streptomyces* sp.# 9885.[1a] WS9885B was later renamed FR182877, and the absolute configuration of this substance was reported to be enantiomeric to the structure illustrated for **1**.[1b−d] This error was corrected in a subsequent publication, and **1** represents what is now the accepted absolute configuration.[1e] FR182877 possesses a hexacyclic architecture containing 12 stereogenic centers and a vinylogous carbonate embedded in a fused 6−6−7 ring system.

A closely related natural product, hexacyclinic acid (**2**), also isolated from *Streptomyces*, was reported in 2000 by Zeeck and co-workers.[2] The ring system and carbon connectivity of hexacyclinic acid are identical to those of FR182877; however, differences between the two structures exist mainly in the peripheral functionality and the stereochemistry of the ABC ring fusions. Specifically, the C8 oxygen is acetylated in **2**, the C11 substituent is at the carboxylic acid oxidation state in **2**, the C2−C20 double bond is hydrated relative to that of **1**, and the hexacyclinic acid ring fusions are AB (cis) and BC (trans) as compared to AB (trans) and BC (cis) in FR182877. Due to the structural similarity of these natural products, **1** and **2** are undoubtedly biosynthetically related and have become the defining members of a new class of potential cancer therapeutics.

FR182877 exhibits potent antitumor activity across a number of susceptible cell lines including MCF-7, A549, HT-29, Jurkat,

(−)-FR182877 (**1**)　　　　Hexacyclinic Acid (**2**)
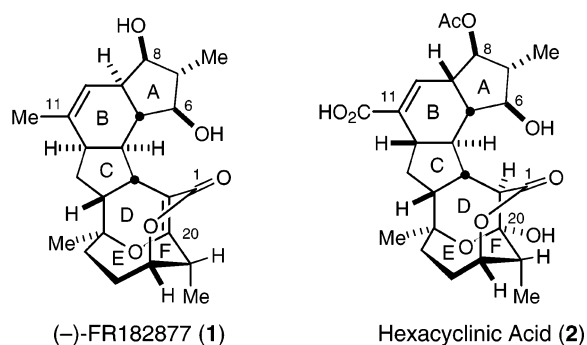
P388, and B16. Results obtained in morphology studies performed with baby hamster kidney (BHK) cells indicate a mechanism of action involving microtubule stabilization and interruption of the cell cycle in metaphase.[1d] As compared to the control (untreated BHK cells), FR182877 performed similarly to Taxol in this assay and, thus, holds forth promise as a new lead structure for the development of antitumor therapeutics that take advantage of this mechanism.

(−)-FR182877 (**1**)　　　　FR182877 oxide (**3**)　　　(1)
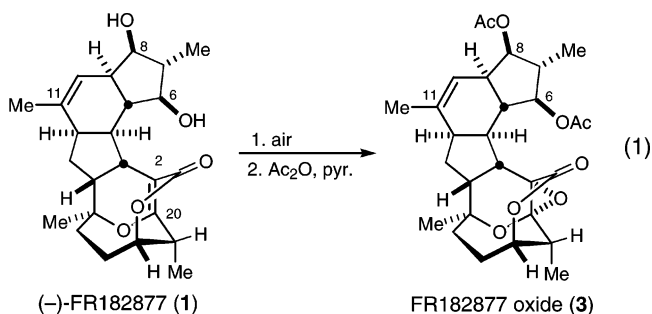
Sato documented the pronounced vulnerability of the strained C2−C20 double bond of **1** to undergo air oxidation to an

(1) (a) Muramatsu, H.; Miyauchi, M.; Sato, B.; Yoshimura, S. 40th Symposium on the Chemistry of Natural Products; Fukuoka, Japan, 1998; Paper 83, p 487. (b) Sato, B.; Muramatsu, H.; Miyauchi, M.; Hori, Y.; Takese, S.; Mino, M.; Hashimoto, S.; Terano, H. *J. Antibiot.* **2000**, *53*, 123. (c) Sato, B.; Makajima, H.; Hori, Y.; Hino, M.; Hashimoto, S.; Terano, H. *J. Antibiot.* **2000**, *53*, 204. (d) Yoshimura, S.; Sato, B.; Kinoshita, T.; Takese, S.; Terano, H. *J. Antibiot.* **2000**, *53*, 615. (e) Yoshimura, S.; Sato, B.; Kinoshita, T.; Takese, S.; Terano, H. *J. Antibiot.* **2002**, *55*, C-1.
(2) Höfs, R.; Walker, M.; Zeeck, A. *Angew. Chem., Int. Ed.* **2000**, *39*, 3258.

epoxide, isolated as the diacetate **3** (eq 1). The epoxide derivative did not appreciably inhibit tumor cell growth, and thus the strained C2−C20 double bond may be necessary for the observed antitumor activity. Hexacyclinic acid displays weak anticancer activity and, in the case of MCF-7 ($GI_{50} = 14 \mu$mol), proved to be 2 orders of magnitude less potent, further implicating the C2−C20 double bond as important for the antitumor activity of this class of compounds. While it is tempting to assign a biologically important role to the strained bridgehead enol ether in **1**, the available examples do not rule out acetylation of the ring-A hydroxyls as the cause of diminished activity in the series.[3]

Interest in the synthesis of FR182877 has risen sharply since its introduction due to its important biological activity as well as its complex polycyclic architecture. Efforts by the Nakada[4] and Armstrong[5] groups have resulted in publications of partial syntheses of the AB ring system and a model of the DF ring system, respectively. The Sorensen group has published two partial syntheses[6a,b] and recently a completed total synthesis[6c,d] of *ent*-**1** nearly contemporaneous with our own communication[7] of the completed synthesis of **1**. In addition to these reports, other research groups are currently investigating syntheses of FR182877.[8]

The unifying theme of the published approaches to **1** has been the disconnection of ring-B using a Diels−Alder cycloaddition transform. The further disconnection of ring-D through a hetero-Diels−Alder cycloaddition was recognized both by us and by Sorensen,[6a] ultimately leading to our independent development of similar syntheses of FR182877 based on a stereocontrolled cascade of transannular Diels−Alder cycloaddition events. In this Article, we provide a complete account of the design and realization of a transannular cycloaddition strategy leading to the completion of a total synthesis of the natural antipode of FR182877. In addition, we describe our efforts to utilize the tools of computational modeling to develop an understanding of the stereochemical outcome of the Diels−Alder cycloaddition cascade.

The hexacyclic structure of **1** incorporates a bridgehead enol ether and an embedded cyclohexene ring, suggesting its biosynthetic origin from a sequence of intramolecular Diels−Alder cycloaddition events. This idea was initially proposed by Sorensen in 1999 and is further supported by the work of Zeeck who isolated isotopically labeled **2** from *Streptomyces* cultures inoculated with ^{13}C-labeled acetate and propionate to establish the connectivity of a supposed polyketide chain precursor to
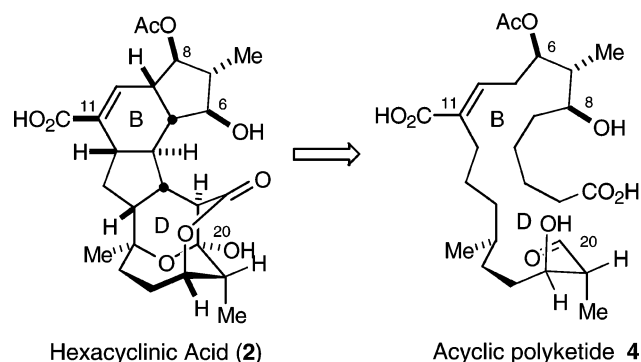

Figure 1. Polyketide origin of hexacyclinic acid.

hexacyclinic acid (Figure 1). This allowed mapping of acetate and propionate subunits to their respective locations in the skeleton of **2** and proved to be consistent with a biosynthetic pathway including Diels−Alder cycloadditions for generating rings B and D.

The structures of **1** and **2** were established by standard spectroscopic methods coupled with X-ray crystallographic analysis, and the absolute configurations were determined in each case by the Mosher ester method. However, on the basis of our own analysis of the reported data for the FR182877 Mosher esters,[9] we suspected that its absolute configuration had been incorrectly assigned. Consequently, we designed a synthesis targeting the configuration of hexacyclinic acid, confident that, in the final analysis, it would prove to be homologous with (−)-FR182877. Our presumption was later confirmed with the publication of a correction in 2002.[1e]

Synthesis Plan. The structural relationship between FR182877 and hexacyclinic acid prompted us to develop a synthesis plan targeting an advanced intermediate bearing the common stereochemical features and peripheral functionality of both natural products. The pivotal transformations associated with both syntheses are the sequential transannular Diels−Alder[10] and hetero-Diels−Alder[11] cycloadditions forming rings B and D, respectively (Scheme 1). Because the ring-B Diels−Alder reaction would be the initiating reaction (see Molecular Modeling section), the **endo-TS** transition state would afford the FR182877 ring system while the diastereomeric **exo-TS** transition state would afford the hexacyclinic acid ring system. We designed macrocycle **5**, carrying a bromine substituent at C11, so that it might serve as a common intermediate for the synthesis of either natural product. In so doing, the syntheses of **1** and **2** could be unified under the common advanced intermediate **5**.

Macrocycle **5** was envisioned to arise from a β-keto ester alkylation and Suzuki[12] cross coupling of the illustrated C3−C10 and C11−C20 fragments. Each fragment could in turn be derived from auxiliary-controlled enolborane syn-aldol

(3) The acetylated pachyclavulariaenones D−F are not cytotoxic, in contrast to potent pachyclavulariaenone G having all three hydroxyls free. Susceptible cell lines were P-388 and HT-29; however, no comment is made on mechanism of action. See: Wang, G.-H.; Sheu, J.-H.; Duh, C.-Y.; Chiang, M. Y. *J. Nat. Prod.* **2002**, *65*, 1475. A comparison of MM2 minimized space-filling models of pachyclavulariaenone G and (−)-FR182877 using Spartan showed considerable homology in size, shape, and disposition of polar functionality between the two natural products (Evans and Starr, unpublished).
(4) Suzuki, T.; Nakada, M. *Tetrahedron Lett.* **2002**, *43*, 3263.
(5) Armstrong, A.; Goldberg, F. W.; Sandham, D. A. *Tetrahedron Lett.* **2001**, *42*, 4585.
(6) (a) Vanderwal, C. D.; Vosberg, D. A.; Weiler, S.; Sorensen, E. J. *Org. Lett.* **1999**, *1*, 645. (b) Vanderwal, C. D.; Vosberg, D. A.; Sorensen, E. J. *Org. Lett.* **2001**, *3*, 4307. (c) Vosberg, D. A.; Vanderwal, C. D.; Sorensen, E. J. *J. Am. Chem. Soc.* **2002**, *124*, 4552. (d) Vanderwal, C. D.; Vosberg, D. A.; Weiler, S.; Sorensen, E. J. *J. Am. Chem. Soc.* **2003**, *125*, 5393.
(7) Evans, D. A.; Starr, J. T. *Angew. Chem., Int. Ed.* **2002**, *41*, 1787.
(8) The following investigators have indicated their efforts toward FR182877 via the Internet: Clarke (http://www.nottingham.ac.uk/~pczpac1/research-web/synthesis.html), Prunet (http://www.dcso.polytechnique.fr/f1-032equipe-.htm).
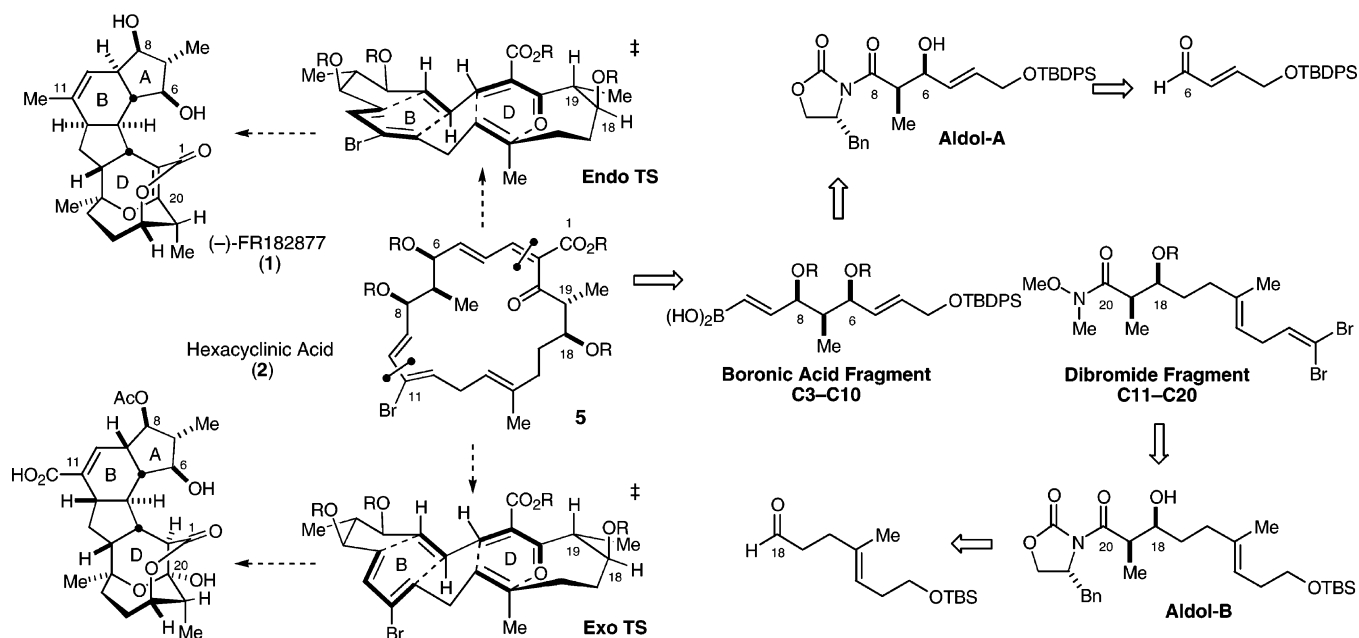
(9) Ohtani, I.; Kusumi, T.; Kashman, Y.; Kakisawa, H. *J. Am. Chem. Soc.* **1991**, *113*, 4092. See also ref 1d for Mosher analysis data on (−)-FR182877.
(10) (a) For a review of TADA reactions, see: Marsault, E.; Toro, A.; Nowak, P.; Deslongchamps, P. *Tetrahedron* **2001**, *57*, 4243. (b) For a recent example, see also: Longithorone A: Layton, M. E.; Morales, C. A.; Shair, M. D. *J. Am. Chem. Soc.* **2002**, *124*, 773. (c) Use of a bromodiene in TADA reaction, see: Roush, W. R.; Koyama, K.; Curtin, M. L.; Moriarty, K. J. *J. Am. Chem. Soc.* **1996**, *118*, 7502.
(11) (a) For this type of hetero-[4+2] cycloaddition, see: Shin, K.; Moriya, M.; Ogasawara, K. *Tetrahedron Lett.* **1998**, *39*, 3765. (b) Takano, S.; Satoh, S.; Ogasawara, K. *J. Chem. Soc., Chem. Commun.* **1988**, 59. (c) Takano, S.; Satoh, S.; Ogasawara, K.; Aoe, K. *Heterocycles* **1990**, *30*, 583. (c) Yamauchi, M.; Katayama, S.; Baba, O.; Watanabe, T. *J. Chem. Soc., Chem. Commun.* **1983**, 281.
(12) For a review, see: Miyaura, N.; Suzuki, A. *Chem. Rev.* **1995**, *95*, 2457.
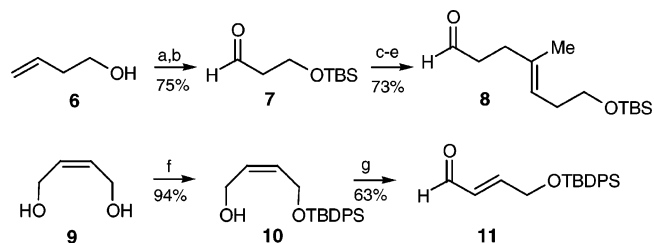
Scheme 1

Scheme 2 [a]

[a] Key: (a) TBSCl, DMF, imid., 90%; (b) O₃/O₂ then PPh₃, 83%; (c) isopropenylmagnesium bromide, THF; (d) triethylorthoacetate, propionic acid, 150 °C, 75% (two steps); (e) DIBAL, CH₂Cl₂, −78 °C, 97%; (f) ⁿBuLi, THF, TBDPSCl, 94%; (g) SO₃−Pyr, DMSO, CH₂Cl₂, TEA, 63%.

reactions[13] affording intermediates, designated as **Aldol-A** and **Aldol-B**, from the appropriately functionalized aldehyde precursors.

Results and Discussion

The Aldol Fragments. The synthesis began with the syntheses of the two obligatory aldehyde fragments (Scheme 2). Silylation of 3-buten-1-ol (**6**) (TBSCl, imidazole, DMF, 90%) was followed by ozonolysis and in situ reduction of the ozonide with PPh₃ to provide an 83% yield of aldehyde **7**. Addition of this aldehyde to a freshly prepared solution of isopropenylmagnesium bromide gave the derived allylic alcohol that was subjected to the Johnson Orthoester Claisen procedure to give the expected ester. The desired aldehyde **8** was then obtained by DIBAL reduction (73%, three steps). Aldehyde **11** was synthesized in two steps from *cis*-2-buten-1,4-diol (**9**). Monosilylation of this diol (TBDPSCl, BuLi, THF, 94%)[14] afforded monosilyl ether **10** which underwent Parikh−Doering oxidation (SO₃−Pyr, TEA, DMSO, CH₂Cl₂, 63%)[15] to give the desired α,β-unsaturated aldehyde **11** after spontaneous cis−trans isomerization during the oxidation procedure.[16]

Synthesis of C11−C20 "dibromide fragment" **17** began with an aldol addition of the enolborane derived from (*R*)-4-benzyl-*N*-propionyl-2-oxazolidinone (**12**) to aldehyde **8** to give syn aldol

adduct **13** in 88% yield (Scheme 3).[13] Conversion of **13** to the derived Weinreb amide **14** (Me₃Al, MeNH₂OMeCl, 96%), silylation of the secondary hydroxyl (TBSCl, 96%), then desilylation of the primary hydroxyl (1:4 TsOH/ⁿBu₄NHSO₄, MeOH, 89%) gave primary alcohol **15**. Successive oxidation (DMP, 94%)[17] to aldehyde **16** and Corey−Fuchs olefination (CBr₄, PPh₃, 74%)[18] afforded the dibromide fragment **17**.

Scheme 3 [a]
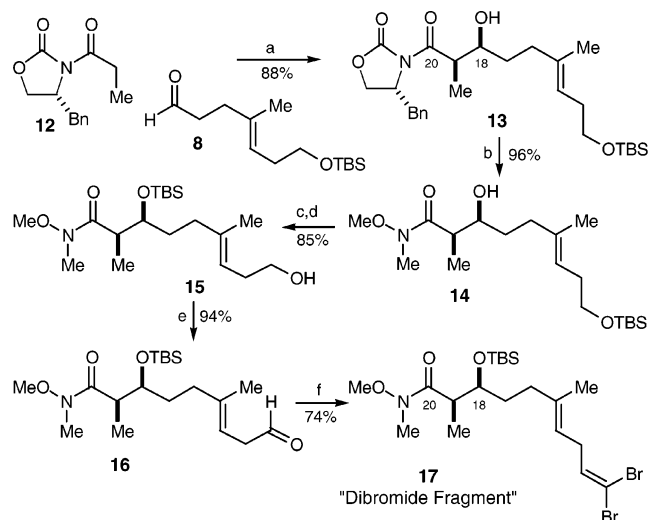
[a] Key: (a) Bu₂BOTf, TEA, 88%; (b) MeNHOMe−HCl, Me₃Al, THF, 96%; (c) TBSCl, DMF, imid., 96%; (d) TsOH:ⁿBu₄NHSO₄ (1:4), MeOH, 0 °C, 89%; (e) DMP, NaHCO₃, 94%; (f) CBr₄, PPh₃, CH₂Cl₂, NaHCO₃, 74%.

The synthesis of the C3−C10 "boronic acid fragment" **23** began with the illustrated aldol addition to provide the expected

(13) Gage, J. R.; Evans, D. A. *Org. Synth.* **1990**, *68*, 77; *J. Am. Chem. Soc.* **1981**, *103*, 2127.

(14) Roush, W. R.; Reilly, M. L.; Kogama, K.; Brown, B. B. *J. Org. Chem.* **1997**, *62*, 8708.

(15) Anderson, J. C.; McDermott, B. P. *Tetrahedron Lett.* **1999**, *40*, 7135.

(16) Complete cis−trans isomerization was observed after storing the neat unpurified reaction product for 24 h.

(17) Dess, D. B.; Martin, J. C. *J. Am. Chem. Soc.* **1991**, *113*, 7277.
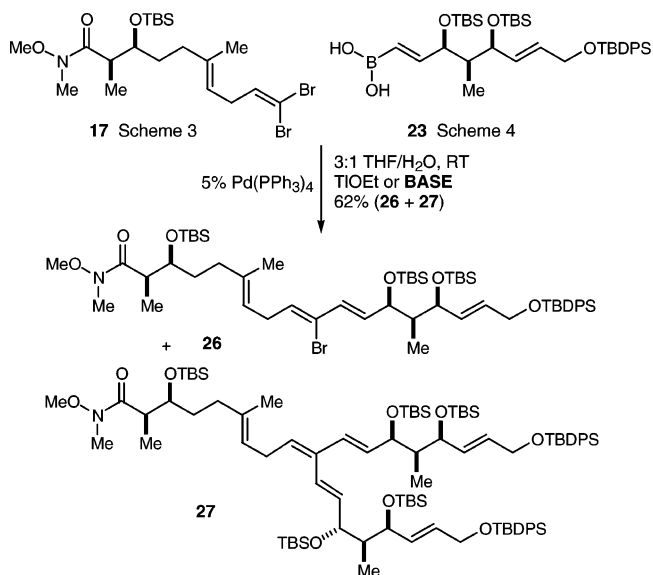
Scheme 4[a]
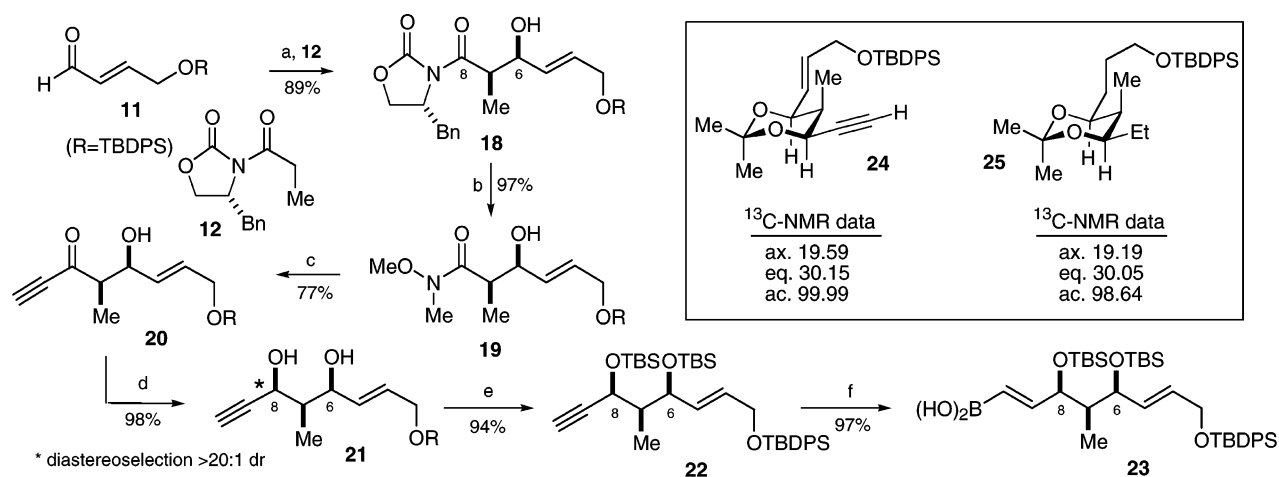
[a] Key: (a) Bu$_2$BOTf, TEA, 89%; (b) MeNHOMe−HCl, Me$_3$Al, THF, 97%; (c) HCCMgBr, 77%; (d) DIBAL, THF, −78 °C, 98%, >20:1 dr; (e) TBSCl, DMF, imid., 98%; (f) Catechol-BH, Cy$_2$BH (0.1 equiv), THF, then 1 N NaOH; 97%.

syn aldol adduct **18** in 89% yield (Scheme 4). The conversion of **18** to amide **19** (Me$_3$Al, MeNH$_2$OMeCl, 97%) was followed by ynone formation (HCCMgBr, 77%) to give acetylenic ketone **20**. Diastereoselective syn reduction using Kiyooka's method (DIBAL, THF, >20:1 dr, 98%)[19] afforded the syn diol **21**. In contrast, reduction of **20** with DIBAL in either Et$_2$O or CH$_2$Cl$_2$ afforded a modest 4:1-syn diastereoselectivity. The relative configuration of **21** at C8 was established by an examination of the ^{13}C NMR chemical shifts of the acetonide carbons of derivative **24** (Scheme 4).[20] The relevant shifts were within accepted ranges for the syn diol isomer. The same analysis was also carried out on the fully saturated analogue **25** to rule out any influence on the result by the adjacent alkyne substituent.[21] Double silylation (TBSCl, 94%) of **21** was followed by alkyne hydroboration using the Arase procedure (catecholborane, catalytic Cy$_2$BH) and saponification (1 N NaOH, 97%) to give the desired boronic acid fragment **23**.[22]

Fragment Coupling. Suzuki coupling of the C3−C10 (**17**) and C11−C20 (**23**) fragments according to the TlOEt-mediated procedure described by Roush[23−24] was initially complicated by the unexpected formation of the doubly coupled product **27** as a substantial side reaction (Scheme 5). With TlOEt, the desired coupling product **26** and side product **27** were obtained in a disappointing 2:1 ratio. Interestingly, the regioisomeric monocoupled product was not observed, suggesting that **27** forms primarily through further reaction of **26** as its concentration builds over time and not through a parallel pathway involving the regioisomer. It is well known through the work of Roush, Kishi,[25] and others[26] that the course of this cross-coupling reaction is greatly influenced by the choice of base. In this reaction, strongly basic conditions (hydroxides or oxides) or less halophilic cations (Na$^+$, K$^+$, Mg^{2+}, Ba^{2+}) were deleterious to the relative rates of reaction, and competitive decomposi-

tion of the starting materials **17** and **23**. Products of protodeborylation, oxidation, and elimination of the C8 silyloxane in **23** typically exceeded 20% yield from these reactions. Dibromide **17** also decomposed, although the product(s) of that pathway could not be identified. Silver bases completely decomposed the starting materials with no return of products **26** or **27**. Carbonate bases improved selectivity for the desired coupling product **26**, but only Tl$_2$CO$_3$ retained a reasonable rate of reaction at room temperature.[27] Ultimately, Tl$_2$CO$_3$ became the base of choice, and, using the improved conditions, Suzuki coupling of **17** and **23** (Tl$_2$CO$_3$, Pd(PPh$_3$)$_4$) afforded bromodiene **26** in 84% yield.

Scheme 5

The completion of the synthesis of the pivotal macrocyclic intermediate **32** is summarized in Scheme 6. Partial reduction of Weinreb amide **26** afforded the corresponding aldehyde (DIBAL), which was subjected to a two-carbon Roskamp homologation (ethyl diazoacetate, SnCl$_2$, 70%, two steps)[28] to give β-keto ester **28**. Selective removal of the TBDPS group

(18) Corey, E. J.; Fuchs, P. L. *Tetrahedron Lett.* **1972**, 3769.
(19) Kiyooka, S.-i.; Kuroda, H.; Shimasaki, Y. *Tetrahedron Lett.* **1986**, *27*, 3009.
(20) Evans, D. A.; Rieger, D. L.; Gage, J. R. *Tetrahedron Lett.* **1990**, *49*, 7099.
(21) Rychnovsky, S. D.; Rogers, B.; Yang, G. *J. Org. Chem.* **1993**, *58*, 3511.
(22) Arase, A.; Hoshi, M.; Mijin, A.; Nishi, K. *Synth. Commun.* **1995**, *25*, 1957.
(23) Use of TlOEt: Frank, S. A.; Chen, H.; Kunz, R. K.; Schnaderbeck, M. J.; Roush, W. R. *Org. Lett.* **2000**, *2*, 2691.
(24) First Suzuki coupling with vinyldibromide: Roush, W. R.; Riva, R. *J. Org. Chem.* **1988**, *53*, 710.
(25) Uenishi, J.; Beau, J. M.; Armstrong, R. W.; Kishi, Y. *J. Am. Chem. Soc.* **1987**, *109*, 4756.
(26) Zhang, H. C.; Chan, K. S. *Tetrahedron Lett.* **1996**, *37*, 1043.

(27) Use of Tl$_2$CO$_3$: Marko, I. E.; Murphy, F.; Dolan, S. *Tetrahedron Lett.* **1996**, *37*, 2507.

Scheme 6 [a]
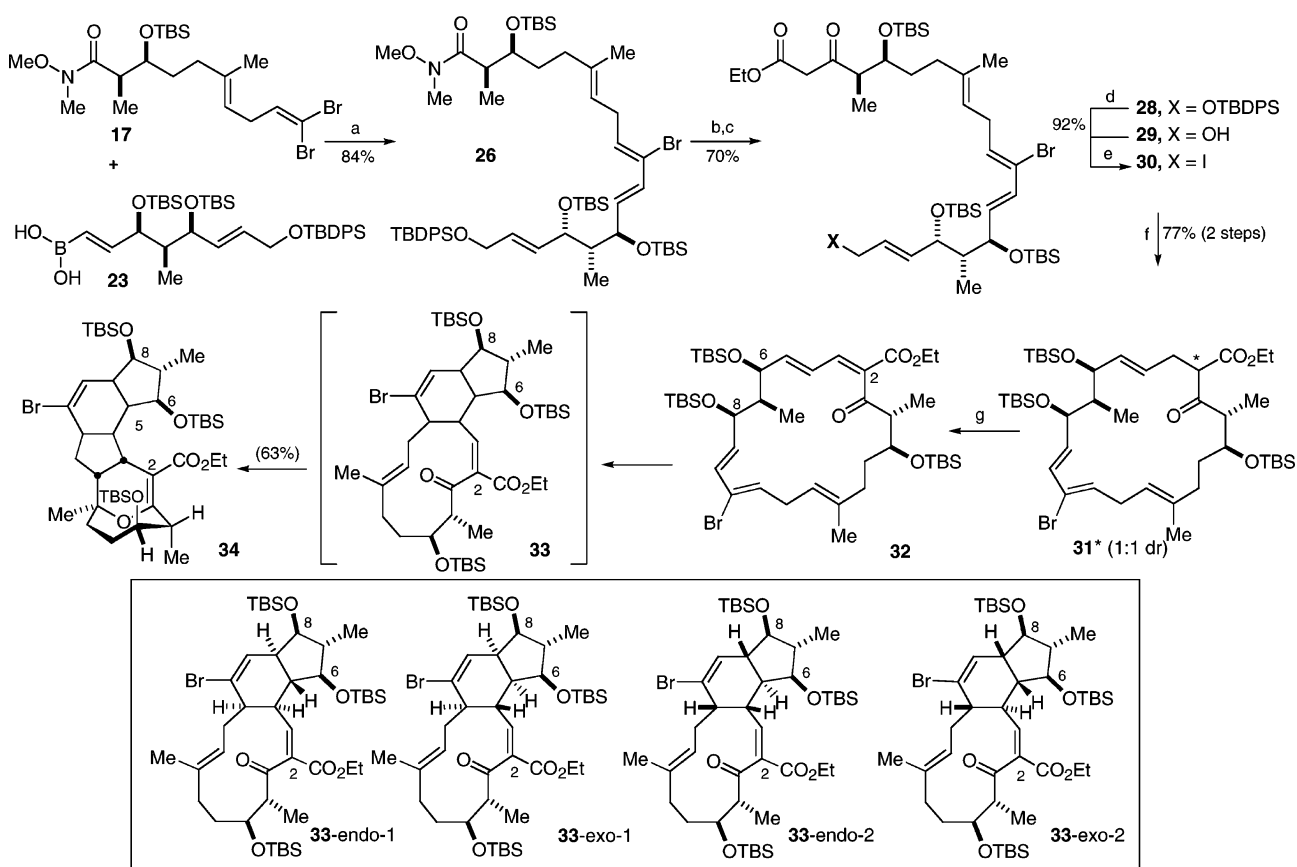
[a] Key: (a) Pd(PPh$_3$)$_4$ (0.05 equiv), Tl$_2$CO$_3$, H$_2$O−THF (1:3), 23 °C, 84%; (b) DIBAL, CH$_2$Cl$_2$, −78 °C; (c) ethyldiazoacetate, SnCl$_2$, 70% (two steps); (d) TBAF, AcOH, DMF, 92%; (e) I$_2$, PPh$_3$, CH$_2$Cl$_2$; (f) Cs$_2$CO$_3$, THF (0.005 M), 23 °C, 77% (two steps); (g) Ph$_2$Se$_2$O$_3$, SO$_3$−Pyr, TEA, THF, 23 °C then hexanes, 50 °C, 63%.

(^{n}Bu$_4$NF hydrate, HOAc, DMF, 92%)[29] provided macrocyclization precursor **29** which was iodinated (I$_2$, PPh$_3$) to afford the sensitive allyl iodide **30** that was immediately submitted to macrocyclization conditions (Cs$_2$CO$_3$, THF, room temperature, 77%, two steps) to give macrocycle **31** as an inconsequential 1:1 mixture of C2 diastereomers.[30]

It was correctly anticipated that intermediate **31**, lacking the C2−C3 double bond, would not engage in a spontaneous transannular Diels−Alder reaction. Oxidation of **31** (Ph$_2$Se$_2$O$_3$, SO$_3$−pyr, TEA, THF, room temperature then 50 °C) initiated a sequence of transannular cycloadditions culminating in the formation of **34** as a single diastereomer as the only isolable product in 63% yield (Scheme 6). Our choice of this particular reagent for the C2−C3 oxidation was based on Deslongchamps' observation that high selectivity was observed in the oxidation of a similar macrocycle.[31]

The transformations leading from **32** to **34** are believed to follow the sequence of events illustrated in Scheme 6. After oxidation of the C2−C3 bond in macrocycle **31**, the targeted macrocycle **32** spontaneously undergoes a normal electron-demand ring-B Diels−Alder cycloaddition to form tricycle **33** followed by an inverse electron-demand hetero-Diels−Alder cycloaddition to give the observed pentacyclic product **34**. The high stereoselectivity of the transannular cycloaddition cascade became apparent upon comparison of the olefinic regions of the ^{1}H NMR spectra of the starting material **31** and product **34** of the reaction. While **31** displays six olefinic methine signals, the oxidation-cycloaddition sequence afforded a product with

only one olefinic methine having a characteristic chemical shift for a nonconjugated halogenated double bond (δ 5.89 ppm). The course of this reaction sequence was monitored by thin-layer chromatography (TLC). During the selenium-based oxidation step, **31** was rapidly transformed (<1 h) to a new species, believed to be **32** that further reacted to form the product **34**. Attempts to isolate **32** as a discrete entity were unsuccessful; however, the unpurified ^{1}H NMR spectrum of the isolation attempt revealed a complex collection of resonances consistent with a ca. 1:1 mixture of **32** and **32′** (eq 2). Signals consistent with the tricyclic intermediate **33** were never observed, suggesting the hetero-Diels−Alder cycloaddition is faster than the normal ring-B Diels−Alder process. Further interpretation of the spectrum was complicated by the presence of several equivalents of selenium reagent and associated byproducts as well as amine salts.

The presence of the 2-H pyran **32′** was not unexpected because vinylogous β-keto esters are known to undergo revers-

(2)

(3)
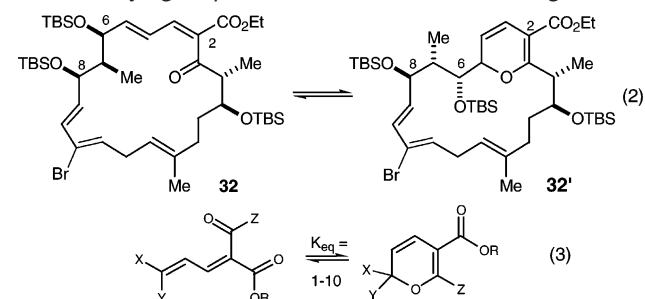
ible 6-π cyclization to give the corresponding 2-H pyrans (eq 3). Moorhoff has documented the relationship between substitution at the X, Y, and Z positions and the observed equilibrium constant for the formation of the pyran tautomer (eq 3).[32] In general, these equilibria ranged between $K_{eq} = 1-10$. If the **32** ↔ **32′** equilibrium is in fact intervening, then the subsequent heating (50 °C) is sufficient to establish a reversible 6-π cyclization-ring opening, thus channeling the reaction cascade through monocyclic intermediate **32**.
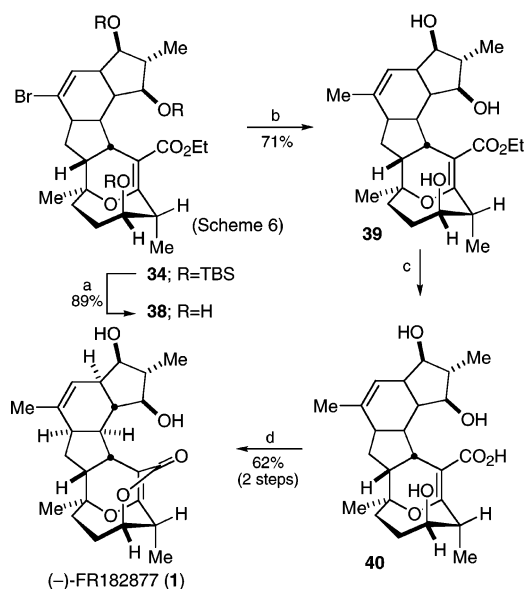
In an attempt to more thoroughly understand the stereoselectivity of the transannular Diels−Alder cascade, a portion of the post-Suzuki-coupling product **26** (Scheme 6) was diverted to study the inherent diastereoselectivity of the ring-B Diels−Alder cycloaddition. Desilylation of **26** followed by oxidation with Dess−Martin periodinane afforded α,β-unsaturated aldehyde **35a**.[17] Gentle warming (60 °C) of a solution of **35a** in CDCl₃ was monitored periodically by ¹H NMR spectroscopy until complete conversion to a mixture of two new species was observed (ca. 3 h) (Scheme 7). The individual products were isolated, and their structures were determined to be intramolecular Diels−Alder products (**36a** and **37a**) by a combination of COSY and NOESY NMR analysis. In this experiment, very high endo selectivity was obtained with an accompanying poor diastereoface selection (dr 37:63 = **36a**:**37a**). After we had performed this experiment, Sorensen published the results of his own investigation of an analogous intramolecular Diels−Alder reaction in which he also observed complete endo selectivity and poor diastereoface selection.[6b] In Sorensen's experiment, a similar Diels−Alder precursor (*ent*-**35b**) underwent a spontaneous intramolecular cycloaddition to afford a 61:39 ratio of cycloadducts *ent*-**36b** and *ent*-**37b**.

Scheme 7
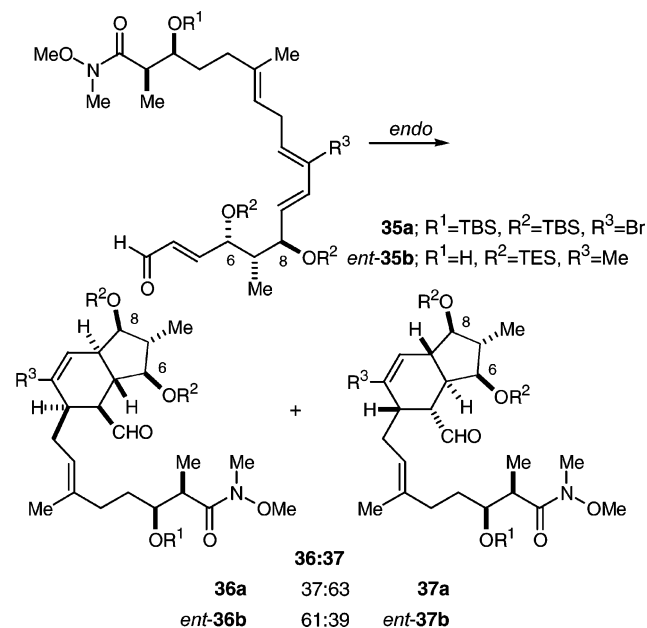
Subsequent comparison of the intramolecular Diels−Alder result (**35a** → **36a** + **37a**) with the transannular Diels−Alder

(28) Holmquist, C. R.; Roskamp, E. J. *J. Org. Chem.* **1989**, *54*, 3258.
(29) Higashibayashi, S.; Shinko, K.; Ishizu, T.; Hashimoto, K.; Shirahama, H.; Nakata, M. *Synlett* **2000**, 1306.
(30) For Cs₂CO₃-mediated macrocarbocyclization, see: Phoenix, S.; Bourque, E.; Deslongchamps, P. *Org. Lett.* **2000**, *2*, 4149.

Scheme 8 *a*

a Key: (a) HF−MeCN, 89%; (b) Me₃B₃O₃, Pd(dppf)Cl (0.1 equiv), Cs₂CO₃, DMF−H₂O (2:1), 100 °C, 71%; (c) TMSOK, THF; (d) Mukaiyama's reagent, NaHCO₃, CH₂Cl₂, 62%.

result (**32** → **34**) (Scheme 6) suggests the C6−C8 stereotriad plays only a muted role in differentiating the reacting π-faces in the ring-B cycloaddition. We suspected this would be the case, given that the particular C6−C8 stereotriad present in **32** is symmetric with respect to the proximal double bonds and, thus, ought to have little differentiating effect upon them. The transannular Diels−Alder strategy was envisioned to amplify the intrinsically small diastereoface selection associated with the C6−C8 triad by transmitting a stereodifferentiating influence through the ring system from the C18 and C19 stereocenters. We believe the resulting high stereoselectivity of the cycloaddition sequence is governed by the stereocenters at C18 and C19 acting through the rigidified macrocyclic architecture to favor a single product of the Diels−Alder cascade. The nature of this influence becomes apparent through computational analysis using simulated transition state structures and is discussed below in the Molecular Modeling section.

COSY and NOESY studies established that the C5 stereocenter in **34** had the desired configuration relative to the C6−C8 triad, but lacked a suitably diagnostic NOESY crosspeak to unambiguously assign the C9 and C12 stereocenters. Because FR-182877 (**1**) and hexacyclinic (**2**) share the C5 stereocenter in common, we could only surmise that **34** must correspond to one of the natural product configurations for the ABC ring system. Comparison of the coupling patterns for the C5−C9 protons in the ¹H NMR spectrum of **34** to the corresponding signals in the ¹H NMR spectrum of aldehyde **36a** obtained in our IMDA study (Scheme 7) provided qualitative evidence that C5 and C9 were trans in **34**, thus corresponding to the FR-182877 ring system. Accordingly, the synthesis of this target was completed by the route outlined in Scheme 8. Global desilylation of **34** (HF−CH₃CN, 89%) afforded triol **38**. This transformation was followed by Suzuki methylation using the procedure of Gray (Me₃B₃O₃, Pd(dppf)Cl₂, Cs₂CO₃, 71%)

(31) Ouellet, L.; Langlois, P.; Deslongchamps, P. *Synlett* **1997**, 689 and references therein.
(32) Moorhoff, C. M. *Synthesis* **1997**, 685.

to give **39**.[33] Saponification of the ethyl ester (TMSOK, THF)[34] yielded seco-acid **40**, and lactonization (1-methyl-2-chloropyridinium iodide, NaHCO₃, 62%, two steps)[35] afforded a white solid whose ¹H NMR and mass spectral characteristics were identical to those published for the natural product **1**. In addition, the ¹³C NMR spectral data also agree to within a 2% margin of error. Finally, synthetic **1** exhibited an optical rotation of $[\alpha_D^{23}] = -5°$ as compared to $[\alpha_D^{23}] = -3.5°$ reported for the natural sample, leading us to conclude that synthetic **1** was of the same absolute stereochemistry as natural (−)-FR182877.

Molecular Modeling

Molecular modeling was used as a tool to address two questions raised during the course of the synthesis described above: (1) In what order do the two transannular Diels−Alder cycloadditions occur? (2) What is the origin of the high diastereoface selection in the normal electron-demand transannular Diels−Alder reaction in the construction of ring-B?

Cycloaddition Order. Simplified macrocycle **32A** was used to calculate the HOMO and LUMO associated with the two Diels−Alder cycloadditions forming the ABCDE ring system (Fgure 2). Calculations were performed using Spartan 5.1 running on an SGI Indigo² computer.[36] The calculated P_z-coefficients of the HOMO and LUMO (for relevant atoms) of **32A** are shown in Figure 2. The best HOMO−LUMO orbital overlap leads to the C4($P_z = -0.26$)−C12($P_z = -0.48$) and C5($P_z = 0.51$)−C9($P_z = 0.38$) bonds, the σ-bonds formed in the ring-B normal electron-demand Diels−Alder (NDA) cycloaddition. The C3($P_z = -0.56$)−C14($P_z = -0.07$) and O1-($P_z = -0.29$)−C15($P_z = 0.03$) combinations associated with the hetero-Diels−Alder (HDA) cycloaddition are considerably weaker due to small HOMO P_z coefficients for the C14−C15 double bond. The π-bonding electron density of C14−C15 is, necessarily, lower lying than that of the C9−C12 diene (HOMO[−1] is 0.11 kcal/mol lower in energy), consistent with the generally higher reactivity of dienes toward electrophilic reagents. This frontier molecular orbital analysis predicts a better HOMO−LUMO overlap for the normal ring-B Diels−Alder reaction than for the ring-D hetero-Diels−Alder process in macrocycle **32**, in accord with the sequence in Scheme 6.
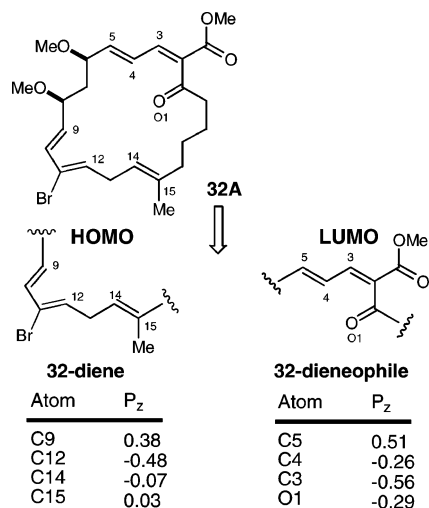

Figure 2. HOMO and LUMO coefficients for macrocycle **32A**.

Ring-B Cycloaddition. The origin of the high observed diastereoface selection in the normal ring-B transannular Diels−
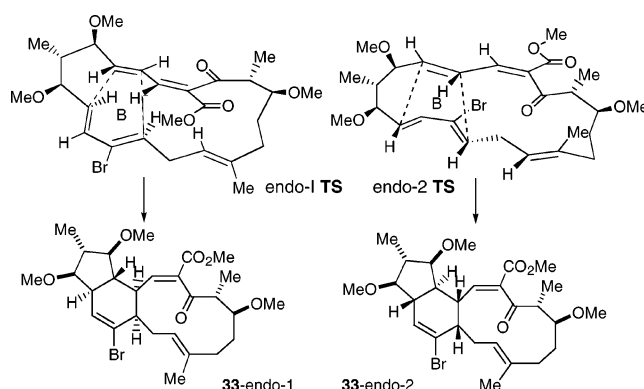

Figure 3. Diagramatic definitions of endo-I and endo-II transition structures.

Alder (TADA) cycloaddition (**32 → 33**) was next examined using semiempirical calculations.[37] The contrast between the poorly face-selective intramolecular Diels−Alder (IMDA) cycloaddition (Scheme 7) and the highly face-selective (TADA) cycloaddition (**32 → 33**) (Scheme 6) reinforces the conjecture that the stereocenters at C18 and C19 are involved in creating the observed TADA face selectivity. This proposal was examined by considering the two endo TADA transition structures **Endo-1 TS** and **Endo-2 TS** (Figure 3). The diene and dienophile termini were constrained at specified distances ranging from 2.9 to 2.1 Å, with energy minimizations (PM3) carried out at 0.2 Å intervals for the two endo cycloaddition geometries. Published Diels−Alder transition state bond distances in the 2.0−2.2 Å range were used in the selection of the internuclear distance constraints.[38] The nine simplified macrocycles (**41−44d**, Figure 4) were minimized with the indicated distance constraints leading either to the observed, natural product (**endo-1 TS**) or to its endo diastereomer (**endo-2 TS**).

For each of the structures **41−44d**, five energy-minimized geometries were obtained, where the interatomic distances between the dienophile (C4 and C5) diene and (C9 and C12) termini were constrained to 2.9, 2.7, 2.5, 2.3, and 2.1 Å. From these data, energy curves (kcal mol⁻¹ Å⁻¹) were generated representing the increasing energy penalty of approaching the transition state. For each macrocycle, two curves were generated: one representing the **endo-1** π-face alignment and the other representing the **endo-2** π-face alignment (Figure 3). The profiles of the two curves generated for each macrocycle were then compared to qualitatively determine which endo approach is preferred by that macrocycle in the TADA cycloaddition. This preference was graphically correlated with the C18 and C19 substituents positioned on the macrocycle.

(33) Gray, M.; Andrews, I. P.; Hook, D. F.; Kitteringham, J.; Voyle, M. *Tetrahedron Lett.* **2000**, *41*, 6237.
(34) Laganis, E. D.; Chenard, B. L. *Tetrahedron Lett.* **1984**, *25*, 5831.
(35) Mukaiyama, T.; Usui, M.; Saigo, K. *Chem. Lett.* **1976**, 49.
(36) The conformational geometry of model **32** was optimized at the PM3 level with the π-conjugated systems constrained to coplanarity using the dihedral constraints outled in ref 37. No interatomic distance constraints were imposed for this experiment. Single point energy and MO coefficients were computed using ab initio methods at the RHF/STO-3G level on the geometry optimized model **32**. All P_x and P_y coefficients were $0 ± 0.05$ for both the HOMO and the LUMO of the indicated atoms.
(37) Dihedral angle constraints were used for all PM3 calculations as follows: O(ester CO)=C1−C2=C3, 180°; C2=C3−C4=C5, 180°; C9=C10−C11=C12, 0°. Interatomic distance constraints were applied to C5−C9 and C4−C12 at distances indicated in the text for the individual experiments.
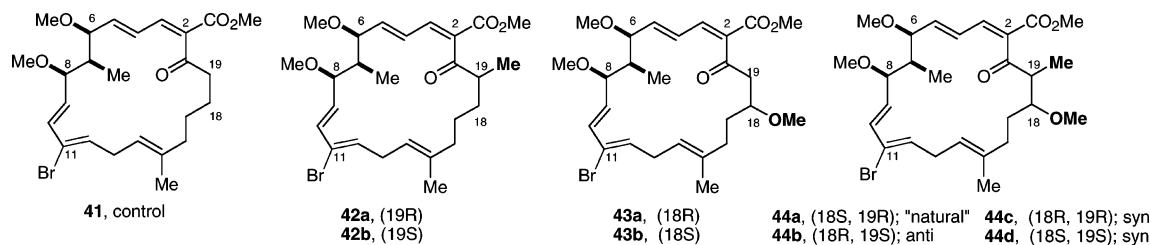(38) Storer, J. W.; Raimondi, L.; Houk, K. N. *J. Am. Chem. Soc.* **1994**, *116*, 9675.

Figure 4. Macrocycles employed for molecular modeling studies.
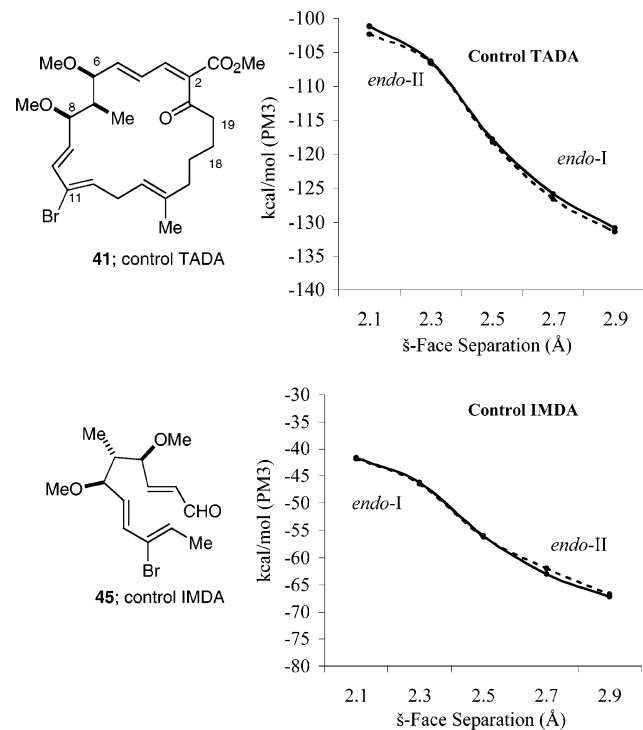

Figure 5. Endo diastereoselection control experiments.

Figure 5 shows the energy curves obtained in a control experiment wherein **41** lacking substitution at both C18 and C19 is evaluated. Only a slight difference in energy (0.5–1.1 kcal/mol) appears between the curves leading to the **endo-1** and **endo-2** transition states. Calculations of the two endo approach curves in a model of the acyclic system **45** produced a similarly small energy difference between the two transition state energy curves, also consistent with the laboratory outcome of the acyclic IMDA and further confirming the negligent impact of the C6–C8 stereocenters in this analysis (Scheme 7).
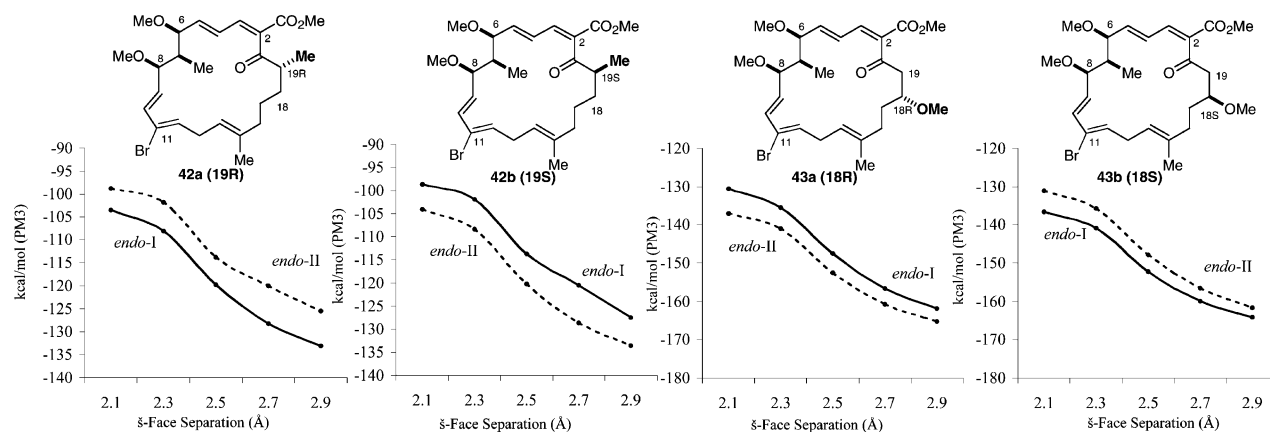
Macrocycles possessing one of the two stereocenters (**42a,b**–**43a,b**) were examined next (Figure 6). The curves generated from **42a** and **42b**, having 19R and 19S methyl configurations, respectively, and no C18 methoxyl substituent, demonstrate a clear bias imparted by the C19 methyl group. Here, the 19R (**42a**) configuration favors the endo-I TS by 4.7–8.2 kcal/mol, while the 19S (**42b**) configuration favors endo-II TS by 5.6–8.1 kcal/mol.

A similar bias is apparent in the curves generated by **43a** and **43b** carrying only the C18 methoxyl substituent (Figure 6). The 18S configuration in **43b** favors the **endo-1 TS** by 2.4–5.5 kcal/mol, while the 18R configuration in **43a** favors the **endo-2 TS** by 3.3–6.5 kcal/mol. This trend suggests that the combination of the two configurations (18S, 19R), the natural configurations found in (−)-FR182877, is reinforcing the **endo-1 TS** π-face alignment observed in the laboratory. Extending this additivity model further, it would be expected that (18R, 19S) would favor the **endo-II** diastereomer while both (18S, 19S) and (18R, 19R) would be nonreinforcing cases with no clear diastereoface preference.

Fully substituted cases **44a**−**44d** were next examined (Figure 7). Energy versus distance plots for these four structures predict that the "natural" (18S, 19R) macrocycle **44a** displays a strong (4.9−9.4 kcal/mol) preference for the **endo-1 TS** in accord with the laboratory outcome. The unnatural (18R, 19S) diastereomeric macrocycle **44b** exhibits a similarly strong preference for the **endo-2 TS** alignment, while macrocycles **44c** and **44d**, (18R, 19R) and (18S, 19S), respectively, deliver less clear-cut results. Macrocycle **44c** modestly favors the **endo-I TS** at larger π-face separations (2.9−2.7 Å). The curves then cross, and the endo-II TS is favored as the π-face separation decreases (2.5−2.1 Å).

Macrocycle **44d**, on the other hand, seems to show no diastereofacial preference for either transition state geometry at the largest π-face separation (2.9 Å); however, at shorter inter-
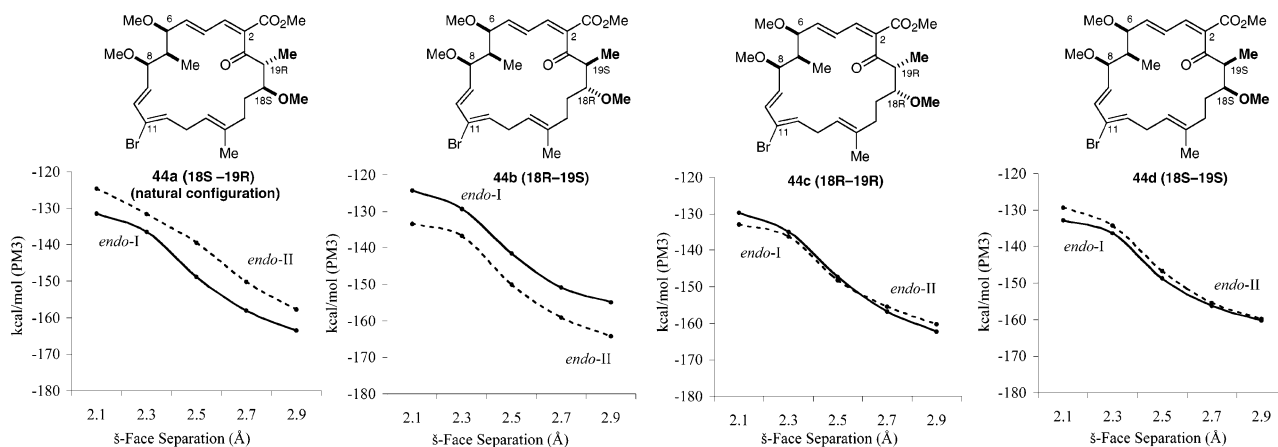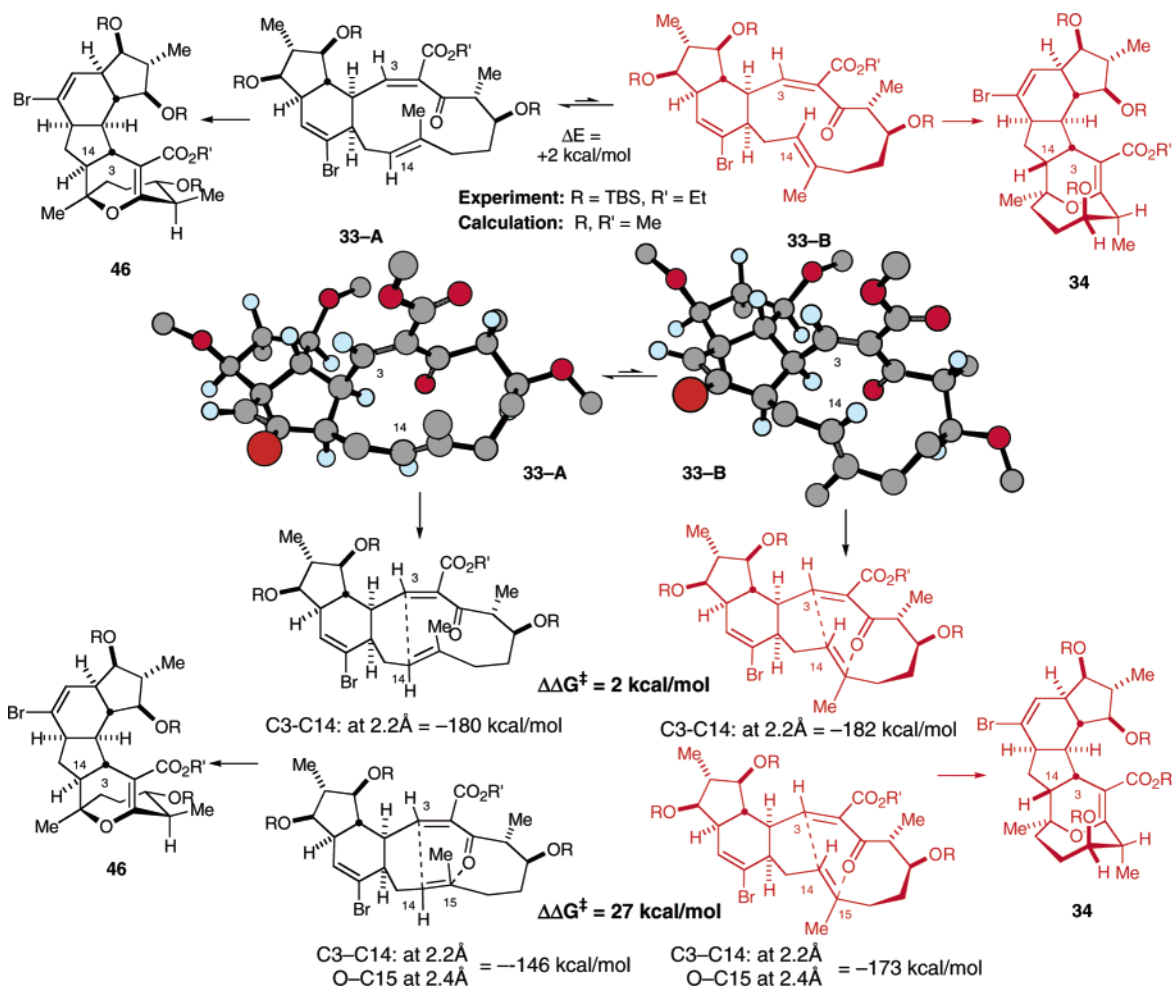

Figure 6. Macrocycles substituted at either C18 or C19.

Figure 7. Macrocycles substituted at both C18 and C19.

Scheme 9

nuclear distances (2.3−2.1 Å), the two curves diverge to favor the **endo-1** transition state, albeit by a smaller margin than was seen for the reinforcing cases. It is apparent from this analysis that the nonreinforcing cases, **44c** and **44d**, confound the diastereoface selection of the TADA cycloaddition, by bringing the two possible endo transition states closer in energy for those diastereomers.

It is noteworthy that the limitation posed by the macrocyclic architecture is primarily the lack of free rotation around the C18−C19 and C19−C20 bonds and the opportunity to alleviate

energetically costly interactions across these bonds. In summary, the computational data and the empirical results implicate both the C18 and the C19 stereocenters as the primary determinants for the diastereoface selectivity of the TADA cycloaddition leading to ring B with the best selectivities being observed in the reinforcing cases (18S, 19R) and (18R, 19S) leading to *endo*-I and *endo*-II, respectively. The preferred *endo*-I transition structure is illustrated in Figure 8. As stated earlier,[37] constraints on dihedral angles, $\varnothing_1$, $\varnothing_2$, and $\varnothing_3$, were imposed on the calculations, while no constraint was imposed on the
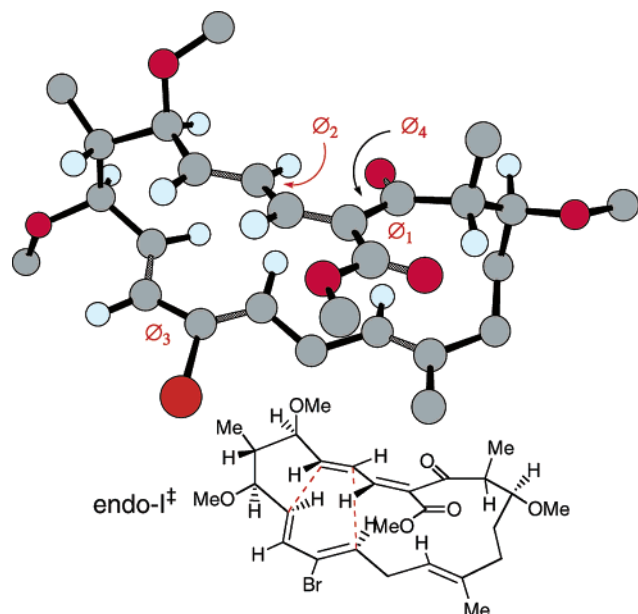
Figure 8. Preferred ring-B Diels−Alder transition state.

intra-annular dihedral angle $\varnothing_4$ linking the ketone carbonyl to the dienophile π-system. Nonetheless, the preferred ring conformation permits conjugation of this carbonyl moiety to the π-system.

The analysis of the hetero-Diels−Alder cycloadditions is provided in Scheme 9. The tricyclic intermediate, formed as a consequence of the first cycloaddition, exists in the two low-energy conformations **33-A** and **33-B** differing in energy by 2 kcal/mol. The more stable conformer **33-A** is the kinetic conformation that evolves from the first cycloaddition, while conformation **33-B** is the obligatory conformation for the desired hetero-Diels−Alder process leading to **34**. As can be seen by the three-dimensional structures, the two macrocyclic conformations only differ in the region C13−C17 where the two diastereofaces of the Δ15 trisubstituted olefin are oriented toward the transannular heterodiene. If no conformational interconversion were possible, the cycloaddition cascade would have probably led to the undesired adduct **46**. Experiment tells us that conformational interconversion must have occurred.

We next carried out calculations to estimate the relative energies of the hetero-Diels−Alder cycloaddition steps. In the first instance, we applied only a single-bond constraint (2.20 Å) between the forming C3−C14 bond. This scenario leads to a carbocation intermediate. In this instance, the desired cycloaddition mode is favored by 2 kcal/mol. In the more realistic situation, we applied an additional bond constraint (2.40 Å) between the C14 and carbonyl component in the heterodiene. When both transition state bond constraints are applied, the cycloaddition mode leading to the desired product is favored by 27 kcal/mol!

Scheme 10
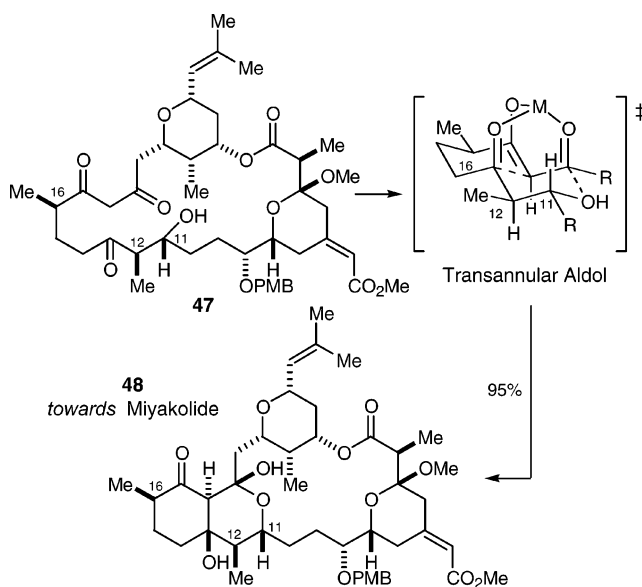
Conclusion

There are numerous examples of complex cycloaddition reactions that occur during the biosynthesis of a broad spectrum of natural products.[39] Some of these transformations are enzymatically mediated, while others need not be so controlled. Rather, the stage could be set for a complex series of transformations that are mediated by internal control elements such as resident stereocenters within the molecular architecture. Such appears to be the case with FR182877.

A related example serves to illustrate this point (Scheme 10). Our group had previously exploited a transannular C−C bond forming reaction in the synthesis of miyakolide.[40] In this synthesis, three stereocenters on the advanced macrocyclic intermediate **47** preorganized the transition state of the transannular aldol reaction **47** → **48** to impart a high degree of stereocontrol to the ensuing reaction. Again, the synthesis activity demonstrates that enzyme mediation of this aldol step is not obligatory.

Supporting Information Available: Experimental details and analytical data for all new compounds (PDF). This material is available free of charge via the Internet at http://pubs.acs.org.

JA037643+

(39) Stocking, E. M.; Williams, R. M. *Angew. Chem., Int. Ed.* **2003**, *42*, 3078.
(40) Evans, D. A.; Ripin, D. H. B.; Halstead, D. P.; Campos, K. R. *J. Am. Chem. Soc.* **1999**, *121*, 6816.